

History effects and pinning regimes in solid vortex matter

S. O. Valenzuela* and V. Bekeris

*Laboratorio de Bajas Temperaturas, Departamento de Física,
Universidad Nacional de Buenos Aires, Pabellón I,
Ciudad Universitaria, 1428 Buenos Aires, Argentina*

(Dated: October 26, 2018)

We propose a phenomenological model that accounts for the history effects observed in ac susceptibility measurements in $\text{YBa}_2\text{Cu}_3\text{O}_7$ single crystals [Phys. Rev. Lett. **84**, 4200 (2000) and Phys. Rev. Lett. **86**, 504 (2001)]. Central to the model is the assumption that the penetrating ac magnetic field modifies the vortex lattice mobility, trapping different robust dynamical states in different regions of the sample. We discuss in detail on the response of the superconductor to an ac magnetic field when the vortex lattice mobility is not uniform inside the sample. We begin with an analytical description for a simple geometry (slab) and then we perform numerical calculations for a strip in a transverse magnetic field which include relaxation effects. In calculations, the vortex system is assumed to coexist in different pinning regimes. The vortex behavior in the regions where the induced current density j has been always below a given threshold ($j_c^>$) is described by an elastic Campbell-like regime (or a critical state regime with local high critical current density, $j_c^>$). When the VS is shaken by symmetrical (e.g. sinusoidal) ac fields, the critical current density is modified to $j_c^< < j_c^>$ at regions where vortices have been forced to oscillate by a current density larger than $j_c^>$. Experimentally, an initial state with high critical current density ($j_c^>$) can be obtained by zero field cooling, field cooling (with no applied ac field) or by shaking the vortex lattice with an asymmetrical (e.g. sawtooth) field. We compare our calculations with experimental ac susceptibility results in $\text{YBa}_2\text{Cu}_3\text{O}_7$ single crystals.

PACS numbers: 74.60. Ge, 74.60. Jg

I. INTRODUCTION

The competition between vortex-vortex interactions and randomness determine the electromagnetic response of type-II superconductors in the mixed state.¹ The interaction between vortices favors an ordered vortex lattice (VL) that opposes the disorder arising from random pinning centers and temperature. The combined effect of these interactions leads to a great variety of collective behaviors, making the VL a paradigmatic system to study an elastic object in a disordered environment.²

The rich static phases of vortex matter in high T_c superconductors have drawn a great deal of attention in the past,^{1,3,4} but recently, much effort has been directed towards understanding vortex lattice dynamics both in low and high T_c materials. Though details are not completely understood, consensus has been reached that the nucleation and annihilation of defects (e.g., dislocations) in the VL might play a major role in its response to an applied force.^{5,6,7,8,9,10,11,12,13,14,15,16} Reproducible states with distinct mobilities have been observed, and it has been argued that this reflects distinct degrees of topological order of the VL: a defective VL would interact more efficiently with pinning centers than an ordered one because of a reduction in its effective shear modulus. In particular, several experiments have revealed that, in certain conditions, an ac magnetic field or an ac current can assist the VL in ordering.^{9,10,11,12,13,14,15,17}

At first, two basic mechanisms have been invoked to account for the dynamic ordering of the VL in low T_c superconductors: a dynamic transition occurring at current densities above a certain threshold^{2,18,19} and an equili-

bration process where an ac magnetic field (or current) perturbation assists the VL in going from a supercooled disordered state into the more ordered equilibrium state. However, data have been reported that can not be accounted for within either of these two frameworks. We refer to the recent findings in the vortex lattice in twinned $\text{YBa}_2\text{Cu}_3\text{O}_7$ (YBCO) single crystals.^{14,15} It was found that when vortices are shaken by a temporarily symmetric ac magnetic field (e.g., sinusoidal), they are driven into a mobile state, but if the shaking field is temporarily asymmetric (e.g., sawtooth), the lattice is trapped into a more pinned structure.¹⁵ As suggested in Ref. 15, the possibility of switching to a high mobility VL state by applying a symmetrical (sinusoidal, square, triangular, etc.) ac magnetic field or to a low mobility VL state by applying a temporarily asymmetric magnetic field waveform (sawtooth, etc.) is inconsistent with a naive equilibration process. In addition, the induced current density that participates in ordering or disordering the VL can be tuned to be comparable by adjusting the magnetic field amplitude and frequency. Disorder observed for higher field sweep rates than those that are used in symmetric oscillating fields that order the vortex lattice is a clear indication that the higher mobility of an ordered VL is not attained through a dynamical transition at high current densities.¹⁵ If this were the case, the VL should also order with the asymmetric ac field that is expected to induce a higher current density.²⁰ This demonstrates, at least for YBCO, that the high or low VL mobility results from a collective dynamical process of a different kind that we believe is intrinsic to the oscillatory motion.

The attained degree of mobility is found to persist af-

ter interrupting the ac excitation for long periods of time (exceeding 1 h). As the ac field penetration is dependent on its amplitude, H_0 , and temperature, T , different regions of the sample may remain in different pinning regimes depending on the detailed thermomagnetic history of the sample.¹⁴ The dynamical rearrangement of the VL occurs in the outer zone of the sample where the penetration of the ac magnetic field induces ac currents that force vortices to move. An increment of H_0 or T will result in an increase in the penetration depth of the ac field. As the ac field further penetrates into the sample, the VL mobility changes. In Ref. 14, we argued that, as long as the current density does not exceed the critical one (so that a small fraction of the vortices moves out of their pinning sites) the VL will remain in the low mobility state. In a bulk-pinning-dominated regime, this will happen in the inner nonpenetrated portion of the sample. As T or H_0 increases this region will shrink and, eventually, disappear. The robustness of the states involved and their spatial distribution in the sample are the main ingredients leading to the observed memory effects in Ref. 14.

In this paper, we present analytical and numerical calculations for the field and current distributions, as well as for the ac susceptibility χ_{ac} in samples with inhomogeneous pinning. If history effects and flux creep can be neglected, the current and flux densities inside the superconductor are often well described by the Bean critical state model²¹ (CS) which assumes a critical current density that is magnetic field independent and a null lower critical field, H_{c1} ($H_{c1} = 0$, $B = \mu_0 H$). Exact analytical solutions have been obtained for the perpendicular geometry^{22,23,24,25,26} which is more appropriate for our experimental arrangement. For more general situations, as in our particular case, a time-dependent theory is required. If it is assumed that the critical current density does not vary over the sample thickness, this dynamic theory can be formulated in terms of a one-dimensional integral equation as discussed by E. H. Brandt.^{27,28} With the use of an appropriate constitutive relation $E(j)$ it is possible to compute the flux motion (and the magnetization) in strips, disks, etc. with homogeneous or inhomogeneous j_c when the applied field is cycled. From the magnetization curves, we calculate the susceptibility. These results are compared with measured ac susceptibility data obtained in a twinned YBCO crystal following a specific protocol to control the spatial pattern of the dynamical behavior of the VL in the sample.

As an example, the VL can be prepared by zero ac field cooling (ZFC), cooling the sample below the critical temperature before applying the magnetic ac field. This traps the VL in a low mobility state¹⁴ with a high critical current density, $\sim j_c^>$. If a sinusoidal ac field is then applied, the VL will become more mobile in the penetrated outer zone of the sample and it will be characterized by a lower critical current density, $\sim j_c^<$. Vortices in the inner region of the sample, where the induced current density j has been always below $j_c^>$, will remain in a

more pinned structure in which vortices oscillate confined in their pinning potential wells.

The critical current patterning so defined may be observed, for example, by removing the ac field and applying an increasing ac probe to measure the ac susceptibility χ_{ac} . This is the basic protocol that we have developed in calculations and in our ac susceptibility measurements to show evidence of the different local degrees of VL mobility. Analytical calculations that qualitatively introduce our model are presented in Section II A. In Section II B we present our numerical calculations of χ_{ac} that take into account a more adequate transverse geometry and also include the effect of flux creep. In calculations, we consider two possible values for the critical current density though it should be kept in mind that it is observed experimentally that j_c depends on the number of cycles of the “shaking” ac field (see Ref. 15). Experimental results are described in Section III and conclusions are drawn in Section IV.

II. THEORY

For symmetrical shaking fields, we can argue that the VL in the inner portion of the sample will remain in a low mobility state as long as the inner current density does not exceed the critical current density. In this case, a Campbell-type regime may describe the elastic pinning of vortices that are confined to oscillate inside a potential well.^{29,30,31,32,33}

The main criterion to discriminate between a Campbell and a critical state regime arises from comparing the scale of the vortex displacement, Δx , produced by the induced currents, and the size of the pinning potential well, r_p . The application of an ac magnetic field results in a periodic compression of the VL, with a maximum effective vortex displacement at the sample’s boundary. This displacement can be easily estimated from the variation of the lattice parameter $a_0 = \sqrt{\frac{2}{\sqrt{3}} \frac{\phi_0}{B_{dc}}}$ that occurs after applying a perturbation in the dc field, B_{dc} . For a sample with no pinning and with $\mu_0 H = B$ (*i.e.*, neglecting H_{c1}), the vortex displacement at the sample perimeter arising from an ac field of amplitude B_0 ($B_0 \ll B_{dc}$) is $\Delta x \approx \frac{1}{2} \frac{B_0}{B_{dc}} R$ where R is the sample radius. If Δx is smaller than r_p the elastic pinning regime usually describes satisfactorily the penetration of magnetic flux. As the ac field amplitude increases, the region in the sample where the elastic regime applies naturally shrinks. We shall come back to this criterion further on, and momentarily we shall address the problem of a superconductor with nonuniform critical current density.

A. Statics. Analytical calculations

We start by calculating the ac susceptibility of an infinite slab ($|x| \leq A$) in a longitudinal magnetic field

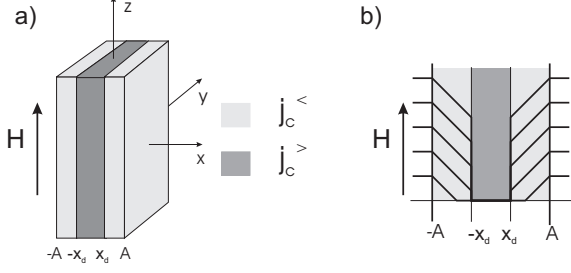


FIG. 1: (a) Infinite slab for $\hat{\mathbf{z}}$ and $\hat{\mathbf{y}}$ used in the estimation of the ac magnetic susceptibility. The field is applied in the $\hat{\mathbf{z}}$ direction. The critical current density is inhomogeneous, with $j_c = j_c^>$ for $|x| < x_d$ (dark gray) and $j_c = j_c^<$ for $|x| > x_d$ (light gray). (b) Field profiles inside the sample for $j_c^> \rightarrow \infty$.

for which the inner critical current density, $j_c^{int} = j_c^>$ ($|x| \leq x_c \leq A$) is larger than the outer one, $j_c^{ext} = j_c^<$ ($x_c < |x| \leq A$) [see Fig. 1(a)]. This first calculation will provide a *qualitative* description of the observed ac field amplitude dependence of the ac susceptibility. We shall not consider at present that the ac field modifies the local critical current density, and we will suppose a given fixed spatial distribution of j_c . For illustrative purposes we also take $j_c^> \rightarrow \infty$ so that the outer region of the sample $x_d < |x| \leq A$ is in the CS whereas there is perfect shielding (Campbell penetration length $\lambda_C \ll x_d$) for $|x| < x_d$. The calculation of χ_{ac} in this simplified situation is straightforward and follows from known results for the critical state in a slab³⁴ if one notes that: *i*) for ac field amplitudes below $H_d = j_c^<(A - x_d)$, χ_{ac} is the well known CS susceptibility for an infinite slab with $j_c = j_c^<$; *ii*) for fields higher than H_d , the sample magnetization is given by the sum of the magnetization due to the outer region of total width $2(A - x_d)$ in the CS and that due to the inner region of width $2x_d$ with perfectly diamagnetic susceptibility $\chi' - i\chi'' = -1$ [see Fig. 1(b)]. For an applied ac magnetic field, $H_{ac} = H_0 \cos(\omega t)$, the susceptibility is

$H_0 \leq H_d$:

$$\chi' = -1 + \frac{1}{2}x \quad (1)$$

$$\chi'' = \frac{2}{3\pi}x \quad (2)$$

$H_0 > H_d$:

$$\chi' = \frac{1}{\pi} \left[\left(\frac{1}{2}x^* - 1 \right) \cos^{-1} \left(1 - \frac{2}{x^*} \right) + \left(-1 + \frac{4}{3x^*} - \frac{4}{3x^{*2}} \right) (x^* - 1)^{1/2} \right] \frac{A - x_d}{A} - \frac{x_d}{A} \quad (3)$$

$$\chi'' = \frac{1}{3\pi} \left(\frac{6}{x^*} - \frac{4}{x^{*2}} \right) \left(\frac{A - x_d}{A} \right) \quad (4)$$

where $x \equiv \frac{H_0}{H_p}$, $H_p = j_c^<A$ and $x^* = \frac{H_0}{H_d} = \frac{H_p}{H_d}x = \frac{A}{A - x_d}x$.

As an example, we plot in Fig. 2(a) the calculated imaginary component χ'' as a function of the normalized ac magnetic field H_0/H_p for different values of x_d/A . These results describe the case of a fixed boundary separating high and low mobility regions of the VL (in each curve the boundary is at a different position). We will address now the more realistic situation where the ac field modifies the position of the boundary.

As was discussed above, the elastic pinning regime is valid for ac fields of low amplitude, where vortex displacements at the sample boundary do not exceed the size of the pinning potential well. As the ac field amplitude is increased, the region in the sample where this condition is valid will be gradually reduced. As a consequence, the curves plotted in Fig. 2(a) for fixed x_d can not be valid for an arbitrary high ac field amplitude. A more realistic approach has to consider that x_d will gradually reduce for sufficiently strong fields. This reduction should be monotonic in the ac field amplitude.

It is useful to define a “minimal penetration susceptibility” that represents the ac susceptibility of a sample that initially contains a homogeneous low mobility VL and is subjected to an increasing ac magnetic field starting from zero. These curves are represented in Fig. 2(a) by dotted lines and will be discussed in the following paragraphs.

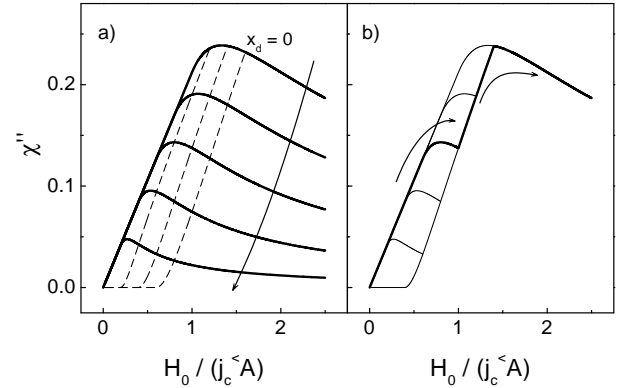


FIG. 2: Dissipative component of the ac susceptibility, χ'' , following Eq. 2 and 4. (a) χ'' vs. $\frac{H_0}{H_p}$ for $x_d/A = 0, 0.2, 0.4, 0.6, 0.8$ (solid thick-lines). The arrow indicates increasing x_d/A . $x_d = 0$ corresponds to the usual critical state. Dotted lines represent the curves of minimal penetration defined in the text for $h_T = 0.2, 0.4$ and $0.6H_p$. (b) Susceptibility for $h_T = 0.4H_p$ and initial $x_d = x_d^i/A = 0.4$ (solid thick-line). The arrows indicate the direction of the magnetic field variation.

The application (in the elastic regime) of a small perturbation field b_s (ac or dc) induces currents that exert a pressure on the vortices at the sample boundary that propagates inside the sample due to the VL elasticity. In a wide slab, the perturbation decays exponentially, with a characteristic length λ_C , the Campbell penetration depth.^{30,31,32,35}

We suppose first an increasing ac field amplitude starting from $H_0 = 0$. As H_0 is increased above a given threshold, h_T , vortices in the outer part of the sample are driven out of the Campbell state as they are forced to move out of their pinning sites. The subsequent oscillatory motion of the vortices produces a reordering of the VL that results in a local reduction of j_c to $j_c^<$. Here, h_T is related to the depth of the pinning potential well in which vortices oscillate in the Campbell regime.

We can estimate x_d as a function of H_0 for a semi-infinite sample ($x \geq 0$). A perturbation b_s penetrates the sample as $\Delta B(x) = b_s \exp(-x/\lambda_{ac})$, where the ac penetration depth is given by $\lambda_{ac}^2 = \lambda^2 + \lambda_C^2$ with λ the London penetration depth.^{35,36} In the case we are interested in $\lambda_C = (c_{11}/\alpha_L)^{1/2}$, where c_{11} is the compressibility of the VL and α_L is the Labusch parameter (in general for weak pinning $\lambda_C \gg \lambda$ and $\lambda_{ac} \sim \lambda_C$).

To determine whether the elastic limit is applicable or not, we estimate the vortex displacement at the sample surface as

$$\Delta x \sim \int_0^\infty \frac{\Delta B(x)}{B_{dc}} dx \quad (5)$$

As discussed above, for displacements $\Delta x \sim r_p$, or larger, the elastic regime is not expected to be applicable. We find from Eq. 5 that this occurs for an applied perturbation $b_s = b_T \sim r_p \sqrt{\alpha_L \mu_0}$, where we have used $\lambda_{ac} \sim \lambda_C$ and $c_{11} \sim B_{dc}^2/\mu_0$ ($b_T = \mu_0 h_T$). If the VL is not strongly perturbed then $\alpha_L r_p = j_c^> B_{dc}$,³⁷ leading to $b_T \propto \sqrt{j_c^>}$.

In the semi-infinite sample, it is evident that this relation establishes the applicability of the elastic Campbell regime at any point inside the sample. Then, we can assume that, if the VL is in a low mobility state ($j_c = j_c^>$) in the whole sample, and the ac field amplitude is increased from zero, x_d will reduce monotonically from $x_d = A$ to a value given by $\Delta B(x_d) = b_T \propto \sqrt{j_c^>}$. In this picture, the ac susceptibility of a slab is given by Eqs. (1)-(4) with x_d not a constant anymore but depending on the applied ac field amplitude,

$$\begin{aligned} H_0 \leq h_T : \quad & x_d = A \\ H_0 > h_T : \quad & x_d = A - \frac{H_0 - h_T}{j_c^<} \end{aligned}$$

Fig. 2(a) shows in dotted lines the “minimal penetration curve” as defined above for the imaginary component χ'' as a function of the normalized ac magnetic field H_0/H_p for $h_T = 0.2, 0.4$ and $0.6 H_p$. In Fig. 2(b), we represent the ac susceptibility of a slab predicted by this simplified picture where the initial state corresponds to a situation in which the vortices in the outer region, $|x| > x_d$, have a higher mobility ($j_c = j_c^<$). In this example, we choose $h_T = 0.4 H_p$ and we show χ'' for different initial values of x_d (x_d^i). The curve represented with a thick line corresponds to $x_d^i = 0.4A$. For $H_0 < H_d$ the internal region of the sample provides no contribution to χ'' , and

the susceptibility corresponds to a slab in critical state. For $H_d < H_0 < H_d + h_T$ (in this example $H_d + h_T = H_p$) χ_{ac} moves away from the CS susceptibility as the internal region contributes with a higher screening capability and the dissipation decreases. However, as $\Delta B(x_d) < b_T$, x_d remains unchanged and equal to its initial value, x_d^i . For $H_0 > H_d + h_T (= H_p)$ the boundary between low and high VL mobility progressively penetrates into the slab and χ_{ac} follows the minimal penetration curve. Finally, for $H_0 = H_p + h_T (= 1.4 H_p)$ the sample is fully penetrated and the CS regime is recovered. The convenience of this calculation will become clear when we describe in Section IV the protocols followed in experiments.

B. Numerical calculations

1. Computational method

The original Bean critical state model has been extended to different geometries, including long strips^{24,26} and circular disks^{22,23,25} in a perpendicular magnetic field. These geometries are more appropriate for our experimental situation. The results obtained analytically can be reproduced by an algorithm developed by E. H. Brandt.^{27,28} The great advantage of the numerical approach is that it allows to analyze static and dynamic problems in samples where the critical current density has a non-trivial dependence on position. The superconductor is modeled by a constitutive law $E(j)$ that has the form $E(j) = E_0 (\frac{j}{j_c})^p$ corresponding to a logarithmic activation energy $U(j) \sim \ln(j_c/j)$ or to $U(j) \sim (j_c/j)^\alpha$ with $\alpha \ll 1$ for a superconductor with critical current density j_c .

Following Brandt, we have considered a strip localized in $|x| \leq d/2 \ll A$ with $|y| \leq A$ and $|z| \gg A$ in an applied field $H_a \hat{\mathbf{x}}$ and we define the sheet current density $\mathbf{J}(y, z) = \int_{-d/2}^{d/2} \mathbf{j}(x, y, z) dx$, which in this case is $\mathbf{J}(y, z) = -J(y) \hat{\mathbf{z}}$ (the extension of these calculations for disks is straightforward and is described in Ref. 28).

The magnetic field generated by these currents is given by Ampère’s law. For the strip, the total field perpendicular to its surface evaluated at $x = 0$ has the form

$$H_x(0, y) = H(y) = \frac{1}{2\pi} \int_{-A}^A \frac{J(u)}{y-u} du + H_a \quad (6)$$

As the current flowing in the strip is induced by the external magnetic field, the symmetry $J(y) = -J(-y)$ can be used in Eq. 6. Considering the electric field $E(y, t) = \dot{\phi}(y, t)/L$, induced by the time dependent magnetic flux $\phi(y) = \mu_0 \int_0^y H(u) du$, one gets an integro-differential equation for the sheet current. This equation has been discretized^{27,28}

$$\dot{J}_i(t) = \sum_{j=1}^N K_{ij}^{-1} \left[\frac{J_j(t)}{\tau} - 2\pi u_j \dot{H}_a(t) \right] \quad (7)$$

where $\tau = \mu_0 a d / (2\pi \rho)$, $\rho = E(j)/j$ and N is the number of points u_i ($0 < u_i < 1$) of the spatial grid, $u_i = u(x_i)$ with $x_i = (i - \frac{1}{2})/N$. In Eq. 7 the strip half width, A , is the unit of length and K_{ij} is given by (see Ref. 27)

$$K_{ij} = \frac{w_j}{N} \ln \left| \frac{u_i - u_j}{u_i + u_j} \right| \quad i \neq j \quad (8)$$

$$K_{ij} = \frac{w_j}{N} \ln \frac{w_j}{4\pi N u_i} \quad i = j$$

where $w_i = u'_i$ is the weight function.

Having obtained the sheet current as a function of time by solving Eqs. (7)-(8), we evaluate the magnetic moment \mathbf{m} of the sample that points in the $\hat{\mathbf{x}}$ direction as

$$\mathbf{m} = \frac{1}{2} \int \mathbf{j} \times \mathbf{r} d^3x \quad (9)$$

which for the strip results in

$$\mathbf{m} = -\hat{\mathbf{x}}ML, \quad M = \int_{-A}^A yJ(y)dy \quad (10)$$

If the applied field is sinusoidal, $H_a(t) = H_{ac}(t) = H_0 \cos(\omega t)$ where $\omega = 2\pi/T$, it is possible to define the ac susceptibility coefficients as

$$\chi'_n = \frac{\omega}{\pi H_0} \int_0^T M(t) \cos(n\omega t) dt \quad (11)$$

$$\chi''_n = \frac{\omega}{\pi H_0} \int_0^T M(t) \sin(n\omega t) dt \quad (12)$$

To obtain the susceptibility we solved Eqs. (7)-(8) by a fourth order Runge-Kutta method with automatic control of the step size.³⁸ We chose the constitutive relation suggested above,

$$\mathbf{E}(\mathbf{J}) = E_c \left(\frac{J}{J_c} \right)^p \frac{\mathbf{J}}{J} \quad (13)$$

with $J = |\mathbf{J}|$.

In the Bean critical state model $E(J)$ is strongly nonlinear and has an abrupt increment at $J = J_c$. For the constitutive relation of Eq. 13 this occurs for $p \rightarrow \infty$. For $1 \ll p < \infty$, it leads to a nonlinear relaxation (approximately logarithmic) of $M(t)$ caused by the nonlinear magnetic flux diffusion. As p decreases the relaxation becomes stronger and in the limit $p = 1$ the behavior is ohmic, with linear magnetic flux diffusion and exponential relaxation of $M(t)$. In our simulations we chose $p = 20$, as $p < 10$ would blur the flux front due to flux

creep and $p > 50$ would require long simulation times to detect relaxation effects. Note that, in general, only the combination E_c/J_c^p is relevant (Eq. 13), and the voltage criterion, E_c , and J_c are not independent. While in the critical state limit E_c is irrelevant, in the ohmic regime $E_c/J_c = \rho$ is the resistivity. Within the dynamical approach that we describe, J_c has a different meaning. As the current is time dependent (it may depend on the rate of variation of the magnetic field), J_c is related to the degree of vortex mobility, where low values of J_c represent highly mobile vortex structures.

The space variable was discretized with $N = 50$ nonequidistant points (results with $N = 30$ showed no significant difference). The tabulation was performed so that the weight function $w(x) = u'(x)$ vanished at the integration boundary to remove the infinity in the integrand occurring at $u \rightarrow 1$ at $t = 0$ (see Ref. 27)

$$u(x) = \frac{3}{2}x - \frac{1}{2}x^3$$

$$w(x) = \frac{3}{2}(1 - x^2)$$

For the ac field $H_{ac}(t) = H_0 \cos(\omega t)$ measured in units of $j_c d$, $\omega = 2E_c/(\mu_0 j_c d A)$ which, in units of $A = 2E_c = j_c d = 1$ is $\omega = 1/\mu_0$. The ac susceptibility was calculated after two complete ac cycles that are necessary to reach a stationary state in the calculation of the hysteresis loop $M[H(t)]$.

2. Current and field profiles. ac susceptibility

In our calculations, the critical sheet current J_c at each point y_i inside the strip depends on the magnetic history of the sample. As was discussed above, we assume that J_c can take two different values, $J_c^>$ or $J_c^<$ (now both finite) depending on the sheet current $J(y_i)$ that flowed in y_i in the previous iteration. For a given H_0 , if $J(y_i) > J_c^>$ then $J_c(y_i)$ is replaced by $J_c^<$ (which has been arbitrarily chosen as unity) and the calculation is restarted. Clearly, the magnetic history of the sample fixes the initial distribution of $J_c(y)$. In Figs. 3 and 4 we show the result of our calculations starting with zero ac field and different initial conditions. In Fig. 3 we show the field (upper panel) and the current (lower panel) distributions for a strip with the following initial critical sheet current distributions: $J_c = J_c^<$ (left), $J_c = J_c^>$ (center), and $J_c = J_c^<$ for $|y/A| \geq 0.75$ and $J_c = J_c^>$ for $|y/A| \leq 0.75$ (right panels).

In the protocol for the calculation of ac susceptibility (Fig. 3) we sweep the ac field from zero. The minimal penetration curve is calculated as follows. We begin with $J_c = J_c^>$ for the whole strip (low mobility initial state, center panels in Fig. 3). The field is increased from zero and we compute the field and current profiles. If the sheet current exceeds $J_c^>$ at any point of the strip, then J_c is changed to $J_c^<$ at that point and the calculations

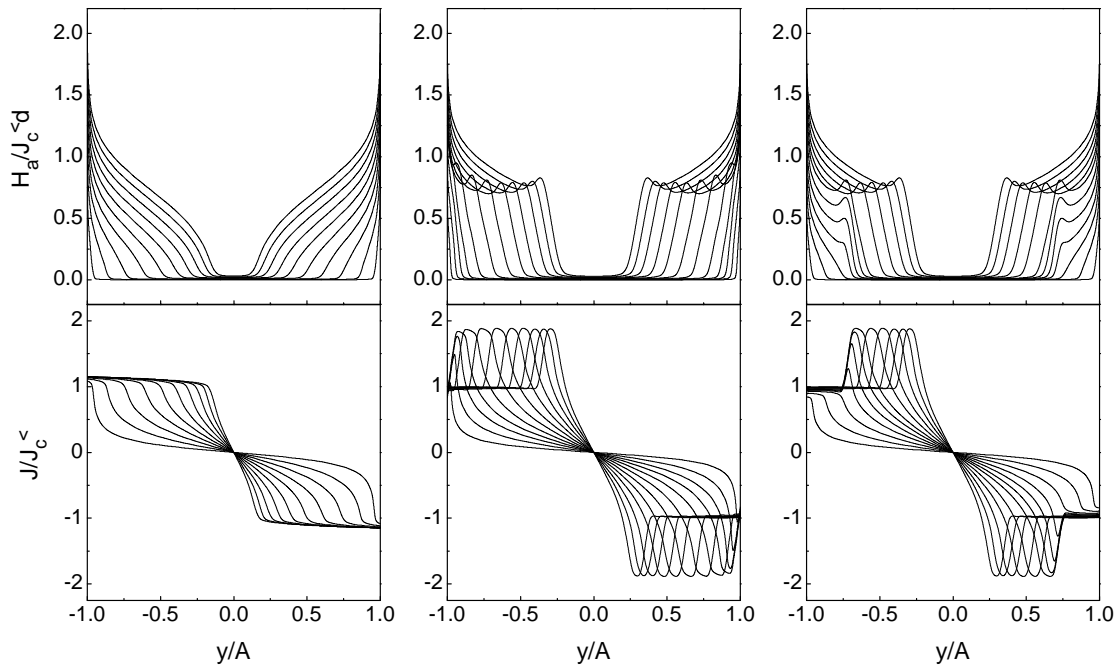


FIG. 3: Field profiles (top) and current profiles (bottom) obtained numerically for a field $H_0 \cos \omega t$ increasing from zero and evaluated at H_0 , for different $H_0 < 1$. Left: homogeneous sample, $J_c^> = J_c^< = J_c$. Center: penetration for the minimal penetration curve $J_c^> = 2J_c^<$. Right: profiles obtained increasing H_0 with initial $x_d^i = 0.75A$. Calculations are for a thin superconducting strip. See the text.

are restarted. This generates by construction the smallest outer region with $J_c = J_c^<$ for each given ac amplitude H_0 (so that $J < J_c^>$ in the whole sample). The field amplitude H_0 is increased again and the procedure repeated. Note that the region with $J_c = J_c^>$ shrinks towards the center of the strip as H_0 is increased. In the calculation of χ_{ac} the field has to be varied in a complete cycle, but it is clear that the critical current density distribution is fixed after the first quarter of cycle.

Now we calculate the rest of the curves that result for a strip with an initial distribution of J_c as in the right panels of Fig. 3. To obtain the initial state, we apply a magnetic field of a given amplitude and we define the initial distribution of J_c following the procedure described above. We then calculate the ac susceptibility increasing H_0 from zero and check for the condition to replace $J_c^>$ by $J_c^<$. This occurs for field amplitudes larger than the one that defined the initial state. Note that from this field amplitude on, the calculated susceptibility coincides with the minimal penetration curve.

It is worth noting that in a strictly 2D model, it is not possible to have an abrupt change in J_c , because this causes a local divergence in J and vortices would always move. To solve this inconvenience, in our calculations, the critical current density changes smoothly from $J_c^>$ to $J_c^<$ over distances of the order of d (where the 2D treatment breaks down²⁵).

In Fig. 4 (left panels) we took $J_c^> = 2J_c^<$. In Fig. 4 (right panels) we compare the minimal penetration curves for different values of $J_c^>$ (1, 1.5 and 2). As we shall see in the next section, the protocol followed in the numerical calculations is particularly convenient to directly compare the numerical results with the experimental ones. In the experiments that are described below, we are able to prepare, in a highly reproducible way, an initial state with low mobility in the whole sample (that is, described in calculations with $J_c^>$) or an initial state with high mobility at the outer region of the sample (a situation that corresponds to $J_c^<$ in the outer region and $J_c^>$ in the inner region).

III. EXPERIMENT

We measured the ac susceptibility of a twinned YBCO single crystal³⁹ using a standard mutual inductance technique. The characteristics of the crystal are: dimensions $0.56 \times 0.6 \times 0.02 \text{ mm}^3$, $T_c = 92 \text{ K}$ and $\delta T_c = 0.3 \text{ K}$ determined by ac susceptibility ($h_{ac}=1 \text{ Oe}$) at zero dc field. In our measurements the ac field is applied parallel to the c axis of the sample. The dc magnetic field $H_{dc} = 3 \text{ kOe}$ was applied at 20° out of the twin boundaries to avoid the Bose-glass phase. Further details can be found in Ref. 14.

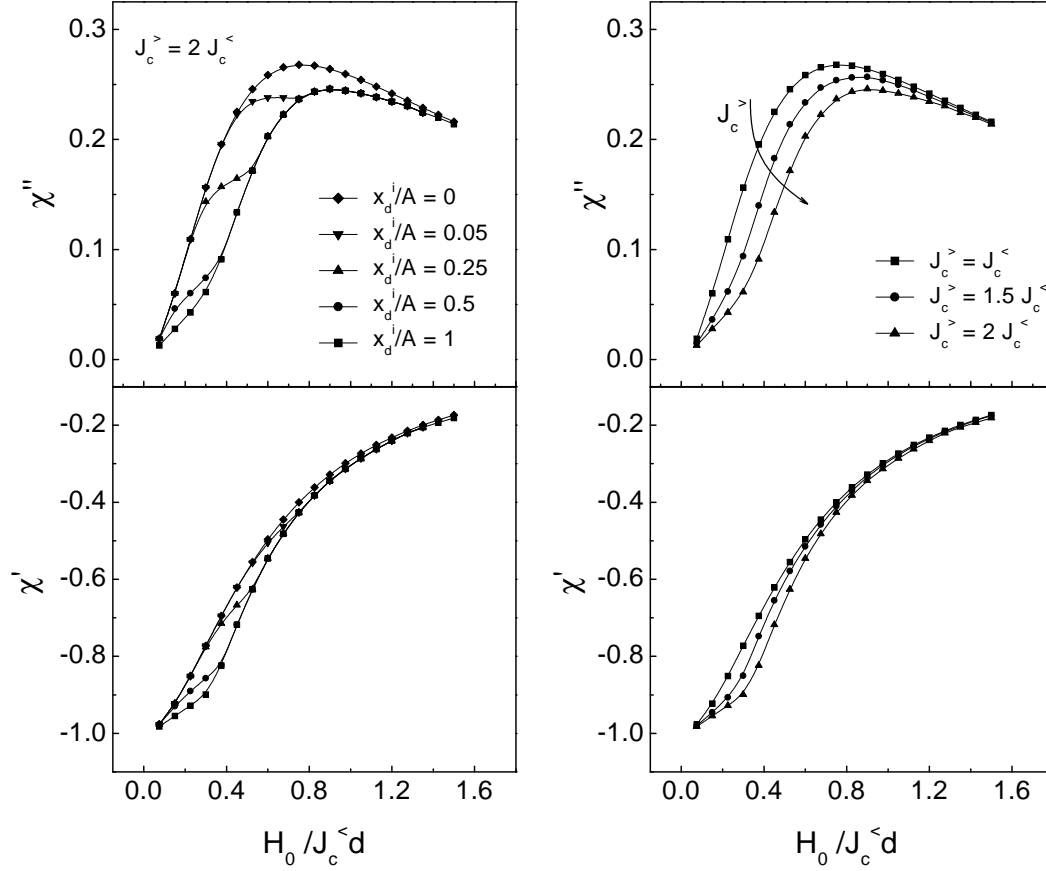


FIG. 4: Numerical calculation of the ac susceptibility of a strip, χ'' (top) and χ' (bottom). On the left, we show results increasing the field for different initial values of x_d , $x_d^i/A = 0, 0.05, 0.25, 0.5$ and 1 . $J_c^> = 2J_c^<$. On the right, we show the minimal penetration curves for $J_c^> = 1, 1.5$ and $2 J_c^<$. They are obtained by taking x_d^i equal to zero. See the text.

The generally unknown dependence of the critical current on temperature makes χ_{ac} measurements vs. ac field amplitude at constant temperature the best choice for comparison with numerical results. The experimental procedure, based on our previous results, is as follows:

- We set the VL in a low mobility state by applying 10^4 cycles of an ac magnetic field with a sawtooth waveform (10 kHz, 8 Oe, see Ref. 15). This field completely penetrates the sample.
- We define the initial state by applying 10^5 cycles of a sinusoidal ac field of a given amplitude at 10 kHz.
- This ac field is turned off and we measure ac susceptibility increasing the amplitude of the ac field probe from zero, with a fixed measuring frequency of 10 kHz.

Results are shown in Fig. 5 for a fixed temperature and $H_{dc} = 3$ kOe. Different initial states were prepared

applying 10^5 cycles of a sinusoidal ac field of amplitudes 0, 1.6, 2.4, 3.2, 4, 4.8 and 8 Oe.

The similarities with numerical simulations for $J_c^> = 2J_c^<$ shown in Fig. 4 are evident. The marked change in the response at the ac field amplitude that defines the initial state supports the scenario of vortices being shaken or not out of the pinning centers on either side of a well-defined boundary. The effective critical current density of the more mobile state can be estimated from the position of the dissipation peak. Comparing Figs. 4 and 5 we have $j_c^< \simeq H_0^{peak}/(0.75d)$. With $d = 30 \mu\text{m}$ and $H_0^{peak} = 3.5$ Oe, $j_c^< \simeq 1250$ A/cm², and thus $j_c^> \simeq 2500$ A/cm² (at 85.2 K).

We also observe that the inductive component does not approach -1 as H_0 is reduced to zero. This is probably a consequence of the finite penetration depth in the Campbell regime.^{29,40} We can determine some of the relevant parameters in this regime, estimating from the saturation value ($\chi'(0) \sim -0.9$), the value for $\lambda_C \sim \lambda_{ac} \sim 10 \mu\text{m}$ ($\gg \lambda \sim 0.6 \mu\text{m}$, Ref. 41) and the size of the potential well $r_p \sim 50 \text{ \AA}$ (Eq. 5 $r_p \sim \lambda_{ac} h_T / H_{dc}$ with $h_T \sim 1.5$ Oe and

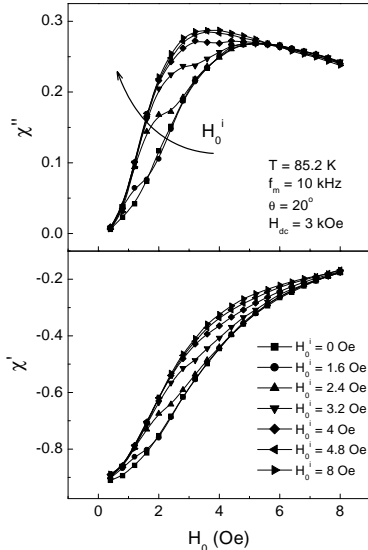


FIG. 5: Experimental results. χ' and χ'' for a YBCO single crystal as a function of the ac field amplitude, H_0 . The measurements were performed increasing H_0 from zero. The different curves correspond to different initial conditions. Before the measurement starts, a low mobility VL is prepared in the whole sample and an ac field of amplitude H_0^i and frequency $f = 10$ kHz is applied to define the initial state. $H_0^i = 0, 1.6, 2.4, 3.2, 4, 4.8, \text{ and } 8$ Oe.

$H_{dc} = 3$ kOe). The value for h_T was estimated as the minimum ac amplitude capable of modifying the measured susceptibility (starting from a low mobility VL).

We note that from these estimates r_p turns out to be of the order of the coherence length $\xi \sim 60 \text{ \AA}$ at our working temperature ($\xi \sim \xi_0(1 - T/T_c)^{-1/2}$ with $\xi_0 \sim 20 \text{ \AA}$, Ref. 41). The Labusch parameter is $\alpha_L \sim \frac{j_c B_{ac}}{r_a} \sim \frac{j_c \phi_0}{r_a} \frac{1}{a_0^2} \sim 10 \text{ N/m}^2 \frac{1}{a_0^2}$ ($100 \text{ dyn/cm}^2 \frac{1}{a_0^2}$).

3. Frequency dependence of the penetration depth

Within the dynamical model described above, an increase in the frequency of the ac field induces a higher ac current (on the average) with a smaller penetration depth. One can gain some insight by considering a stationary state where a constant field ramp \dot{H}_a is applied. In the stationary state the current induced by the field ramp does not change with time and the electric field is obtained as $\nabla \times \mathbf{E} = -\dot{\mathbf{B}}_a$, where $\mathbf{B}_a = \mu_0 \mathbf{H}_a$, implying $E \sim \dot{B}_a$. Inverting Eq. 13 we get $J \sim (\dot{B}_a)^{1/p}$, which shows how J grows as \dot{B}_a is increased. Taking $J = \text{constant}$ in, for example, Eq. 7, we arrive at the same result.

The reduction in penetration due to an increment in the frequency can be deduced using an interesting scaling property of Eq. 7 (Ref. 42). Explicitly, if the unit of time is changed by a factor k and time is expressed as $\tilde{t} = t/k$, then the new functions $\tilde{J}(\tilde{t}) = J(t) k^{1/p-1}$ and $\tilde{B}_a(\tilde{t}) =$

$B_a(t) k^{1/p-1}$ satisfy the same equations. The resulting magnetic field scales with the same factor. If we consider a periodic magnetic field, $H_{ac}(t) = H_0 \sin \omega t$, this scaling property implies that if the frequency is increased by a factor 10 and the ac field amplitude is also increased but by a factor $10^{(1/p-1)}$, the field penetration depth inside the sample will remain unchanged.⁴² This leads to the immediate conclusion that if the frequency is increased but the amplitude of the field is maintained constant, then the penetration depth will be smaller.

This behavior is observed experimentally. In Fig. 6 we compare the imaginary part of the susceptibility measured at 10 kHz after applying 10^5 cycles of a sinusoidal ac field of a given amplitude at 100 kHz [Fig. 6(a)] and at 10 kHz [Fig. 6(b)]. As the amplitude of the measuring field increases, the susceptibility senses the VL mobility in the regions closer to the center of the sample. As the change in the response towards the low dissipation branch is first observed in Fig. 6(a), it is clear that the penetration at 100 kHz is smaller than at 10 kHz. The reason for this is that, in the former case, the high-mobility outer-region is necessarily smaller as implied by the susceptibility measurements (note that the susceptibility is measured at 10 kHz). From this difference, and applying the scaling law discussed above, we can estimate the exponent p in Eq. 13. As an example, the penetration depth of 3.2 Oe at 100 kHz is approximately equal to the penetration of 2.7 Oe at 10 kHz. Assuming a linear dependence of the penetration depth with the ac field amplitude, we obtain $p \sim 15$, which is close to the value we used in our simulations.

4. Temporarily symmetric and asymmetric ac magnetic fields

We have suggested in Ref. 15 that a change in the mobility of the VL may be related to a change in its degree of order, and that these changes are intrinsic to the oscillatory dynamics. Molecular dynamics calculations⁴³ support the scenario where defects are healed by a temporarily symmetric oscillation and created by a temporarily asymmetric oscillation. These simulations also show that the mean velocity of the VL increases as the number of defects decrease.

In the previous section we showed that it is possible to increase vortex mobility (or to order the VL) by applying a temporarily symmetric ac field, and we proved that this reordering occurs in the outer penetrated region of the sample, *i.e.* in the regions where induced currents have densities above the critical current density. We also know that a temporarily asymmetric field produces the opposite effect: it leads the VL into a low mobility (disordered) state.¹⁵ Then, the following questions arise: *i*) Does the penetration depth of the disordered region have a similar dependence on ac amplitude as the penetration depth of the ordered region for symmetrical ac magnetic fields? *ii*) Does the amplitude of the asymmetric field

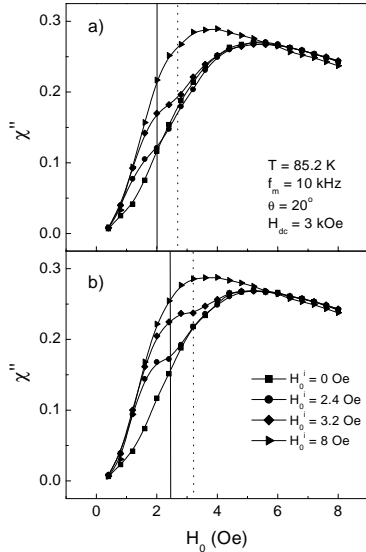


FIG. 6: Experimental results analogous to those shown in Fig. 5. To define the initial state, we applied an ac field with the amplitudes used in Fig. 5 but with frequencies 10 times higher ($f = 100$ kHz)[(a)]. As a comparison we have included results for χ'' from Fig. 5 in panel (b). It is clear that in the latter case the field that defines the initial state (10 kHz) penetrates deeper into the sample. This is because the boundary between low and high critical current densities is found at a higher H_0 when the initial state is defined with 10 kHz as noted by the vertical lines. In other words, the vertical lines compare the corresponding ac field amplitudes for which the measuring field has penetrated inside the sample a length similar to that penetrated by the field that defines the initial state.

have to be above a certain threshold to produce any effect?

Related to this last question we found that, for the application of a symmetrical field, the minimum amplitude that produces some reordering is ~ 1.5 Oe, and this value may be related to the depinning of vortices out of their pinning sites. As we shall see, however, the threshold amplitude for the asymmetric field to produce some disordering is twice as high, thus the process that prevents the VL from switching to a more pinned state should have a different origin.

The experimental protocol for the asymmetric ac fields is very similar to the one described above for symmetric fields, but was modified so that the mobility of the initial state is low. The following procedure is used:

- We generate a high mobility VL in the whole sample by exposing it to 10^4 cycles of an oscillating magnetic field with a sawtooth waveform (8 Oe amplitude and 10 kHz) followed by 10^5 cycles of a sinusoidal ac field of the same amplitude and frequency. This leads to a high mobility VL in the whole sample.
- We define the initial state by applying 10^5 asym-

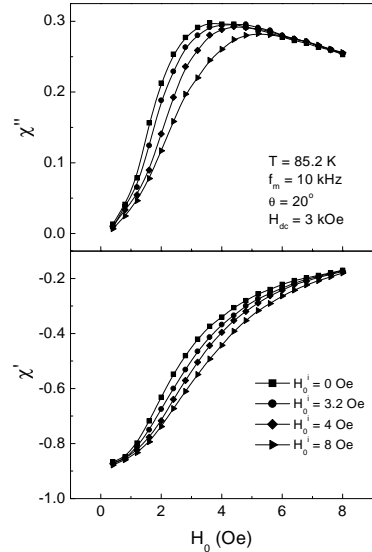


FIG. 7: χ' and χ'' in increasing field for different initial conditions. The mobility of the VL is reduced when asymmetric ac fields are applied. Before the measurement starts, a high mobility VL is prepared in the whole sample and a sawtooth field of amplitude H_0^i and frequency $f = 10$ kHz is applied to define the initial state. $H_0^i = 0, 1.6, 4,$ and 8 Oe.

metric ac magnetic field cycles (*i.e.*, sawtooth) of a given amplitude, H_0^i (10 kHz).

- We measure ac susceptibility with a sinusoidal ac probe as a function of amplitude, starting from amplitude zero (measuring frequency: 10 kHz).

Results are plotted in Fig. 7 for the same temperature and field conditions of Figs. 5 and 6. We investigated different initial states prepared by the application of a sawtooth waveform ac field with amplitude, H_0^i , between 0 and 8 Oe (we show the results for $H_0^i = 0, 3.2, 4,$ and 8 Oe). The first observations are that there seems not to be a clear boundary separating two regions with different vortex mobilities as in Fig. 5, and that changes in susceptibility are important only for $H_0^i \sim 3$ Oe or higher. With asymmetric ac fields, the curves for the different H_0^i resemble the minimal penetration curves of Fig. 4 for different J_c^{int} s. The fact that there is no clear boundary between two regions with associated different mobilities of the VL might be explained by the difference in the sweep rate of the sawtooth waveform that implies a different penetration depth in the ramp up and down of the field. The measuring ac field can also contribute to blur the boundary as it tends to counteract the effect of the sawtooth ac field. On the other hand, we cannot obviate the fact that the shape of the susceptibility does not favor its observation. Finally, another possible explanation for this behavior is related to the mechanism that leads to the decrease of the VL mobility. In Ref. 15, we proposed that this decrease is related to an increase in the density of topological defects due to

plastic distortions in the VL that are produced by the temporarily asymmetric induced currents (cf. Fig. 6, it is implicitly shown that higher field rates induce higher currents). The observation of a minimum amplitude ~ 3 Oe required to produce a strong effect in the mobility of a moving lattice supports this assumption. For plastic distortions to occur, we expect that vortices should move around one lattice parameter. For a sample in the critical state, the displacement at the sample boundary caused by a field that penetrates a distance d is $\Delta x \approx \frac{1}{4} \frac{H_0}{B_{ac}} d$ (for d smaller than the sample radius). For a sample of radius $250 \mu\text{m}$ in a 3 kOe dc field and 3 Oe ac field (6 Oe peak to peak, and 5 Oe of full penetration) the total vortex displacement at the sample periphery is $\sim 0.1 \mu\text{m}$, which is of the order of the lattice parameter $a_0 = 0.09 \mu\text{m}$.

We note that although an important portion of the VL is moving by the application of 3 Oe ac field, only the portion near the sample boundary is initially distorted. This is not what occurs during VL ordering, where all the vortices that move by the action of a symmetrical ac field organize in a more ordered structure. It is possible that the defects generated at the outer region of the sample by the sawtooth waveform diffuse deeper into the sample assisted by the moving lattice. As disorder is produced only for high ac fields ($H_0 > 3$ Oe) that penetrate an important fraction of the sample, a significant portion of the VL will be contaminated after a certain number of oscillations. This description is supported by the direct observation in molecular dynamics simulations⁴³ of the high mobility of dislocations in VL forced by oscillating forces.

IV. CONCLUSIONS

We have presented a phenomenological model that accounts for the history effects in the the ac response of

YBa₂Cu₃O₇ single crystals. The model is based on the effect of inhomogeneous volume-pinning in the ac susceptibility. We obtained analytical expressions for a simple geometry to address qualitatively the details of the model, and then we presented numerical results by solving Maxwell's equations for a more realistic situation.

We presented new experimental results that are adequate for comparison with the numerical calculations. The very good qualitative agreement between them indicates that we have captured the essence of what occurs in relation to the different dynamical responses of the VL inside the sample.

The existence of a threshold sawtooth ac magnetic field amplitude required to lower the VL mobility supports the hypothesis of a ratchet-tearing of the VL produced by temporarily asymmetric fields as was suggested in Ref. 15.

Some of the differences between experimental and numerical results are probably a consequence of an intrinsic property of the experimental technique that undoubtedly perturbs the state of the VL and in a way that may depend on the initial conditions. A sinusoidal ac field increases vortex mobility and the measurement itself can mask the effect of a previously applied asymmetric ac field. Besides, J_c is not restricted to take only two values. Future experimental and theoretical work is required to further understand the oscillatory VL dynamics.

Acknowledgments

VB acknowledges financial support from CONICET. This research was partially supported by UBACyT TX-90, CONICET PID N° 4634 and Fundación Sauberán.

* Present address: Physics Department, Harvard University, Cambridge, MA 02138.

¹ G. Blatter, M. V. Feigel'man, V. B. Geshkenbein, A. I. Larkin, and V. M. Vinokur, *Rev. Mod. Phys.* **66**, 1125 (1994).

² G. W. Crabtree and D. R. Nelson, *Phys. Today* **50**, 38 (1997).

³ E. H. Brandt, *Rep. Prog. Phys.* **58**, 1465 (1995).

⁴ L. F. Cohen and H. J. Jensen, *Rep. Prog. Phys.* **60**, 1581 (1997).

⁵ H. K pfer and W. Gey, *Phil. Mag.* **36**, 859 (1977).

⁶ S. J. Mullock and J. E. Evetts, *J. Appl. Phys.* **57**, 2588 (1985).

⁷ P. H. Kes and C. C. Tsuei, *Phys. Rev. B* **28**, 5126 (1983).

⁸ A.-C. Shi and A. J. Berlinsky, *Phys. Rev. Lett.* **67**, 1926 (1991).

⁹ W. Henderson, E. Y. Andrei, and M. J. Higgins, *Phys. Rev. Lett.* **81**, 2352 (1998); Y. Paltiel, E. Zeldov, Y.N.

Myasoedov, H. Shtrikman, S. Bhattacharya, M.J. Higgins, Z.L. Xiao, E.Y. Andrei, P.L. Gammel and D.J. Bishop, *Nature* **403**, 398 (2000).

¹⁰ Z. L. Xiao, E. Y. Andrei, and M. J. Higgins, *Phys. Rev. Lett.* **83**, 1664 (1999).

¹¹ S. S. Banerjee, N. G. Patil, S. Ramakrishnan, A. K. Grover, S. Bhattacharya, P. K. Mishra, G. Ravikumar, T. V. C. Rao, V. C. Sahni, M. J. Higgins, et al., *Phys. Rev. B* **59**, 6043 (1999).

¹² E. Y. Andrei, Z. L. Xiao, P. Shuk, and M. Greenblatt, *J. Phys. IV* **Pr10**, 5 (1999).

¹³ G. Ravikumar, K. V. Bhagwat, V. C. Sahni, A. K. Grover, S. Ramakrishnan, and S. Bhattacharya, *Phys. Rev. B* **61**, R6479 (2000).

¹⁴ S. O. Valenzuela and V. Bekeris, *Phys. Rev. Lett.* **84**, 4200 (2000).

¹⁵ S. O. Valenzuela and V. Bekeris, *Phys. Rev. Lett.* **86**, 504 (2001).

- ¹⁶ R. Wördenweber, P. H. Kes, and C. C. Tsuei, Phys. Rev. B **33**, 3172 (1986).
- ¹⁷ X. S. Ling, S. R. Park, B. A. McClain, S. M. Choi, D. C. Dender, and J. W. Lynn, Phys. Rev. Lett. **86**, 712 (2001).
- ¹⁸ S. Bhattacharya and H. J. Higgins, Phys. Rev. Lett. **70**, 2617 (1993).
- ¹⁹ A. E. Koshelev and V. M. Vinokur, Phys. Rev. Lett. **73**, 3580 (1994).
- ²⁰ Note that, in the experiments of Ref. 15, the average amplitude of the vortex oscillation is of the order of one lattice constant. In this situation, the steady-motion theory of Ref. 19 is not expected to apply.
- ²¹ C. P. Bean, Rev. Mod. Phys. **2**, 31 (1964).
- ²² J. Zhu, J. Mester, J. Lockhart, and J. Turneaure, Physica C **212**, 216 (1993).
- ²³ P. N. Mikheenko and Y. E. Kuzovlev, Physica C **204**, 229 (1993).
- ²⁴ E. H. Brandt and M. Indenbom, Phys. Rev. B **48**, 12893 (1993).
- ²⁵ J. R. Clem and A. Sanchez, Phys. Rev. B **50**, 9355 (1994).
- ²⁶ E. Zeldov, J. R. Clem, M. McElfresh, and M. Darwin, Phys. Rev. B **49**, 9802 (1994).
- ²⁷ E. H. Brandt, Phys. Rev. B **49**, 9024 (1994).
- ²⁸ E. H. Brandt, Phys. Rev. B **50**, 4034 (1994).
- ²⁹ E. H. Brandt, Phys. Rev. B **50**, 13833 (1994).
- ³⁰ A. M. Campbell, J. Phys. C **2**, 1492 (1969).
- ³¹ A. M. Campbell, J. Phys. C **4**, 3186 (1971).
- ³² A. M. Campbell and J. E. Evetts, Adv. Phys. **21**, 199 (1972).
- ³³ M. Konczykowski, Y. Wolfus, Y. Yeshurun, and F. Holtzberg, Physica A **200**, 305 (1993).
- ³⁴ R. B. Goldfarb, M. Leental, and C. A. Thompson, in *Magnetic Susceptibility of Superconductors and Other Spin Systems*, edited by R. Hein, T. Francavilla, and D. Liebenberg (Plenum Press, New York, 1991), pp. 49–80.
- ³⁵ E. H. Brandt, Physica C **195**, 1 (1992).
- ³⁶ E. H. Brandt, Phys. Rev. Lett. **67**, 2219 (1991).
- ³⁷ E. H. Brandt, J. Low Temp. Phys. **64**, 375 (1986).
- ³⁸ W. H. Press, S. A. Teukolsky, W. T. Vetterling, and B. P. Flannery, *Numerical Recipes in Fortran 77: The Art of Scientific Computing* (Cambridge University Press, 1992).
- ³⁹ I. V. Aleksandrov, A. B. Bykov, I. P. Zibrov, I. N. Makarenko, O. K. Mel'nikov, V. N. Molchanov, L. A. Muradyan, D. V. Nikiforov, L. E. Svistov, V. I. Simonov, et al., JETP Lett. **48**, 493 (1988).
- ⁴⁰ G. Pasquini, Ph.D. thesis, Universidad de Buenos Aires (1998).
- ⁴¹ C. P. Poole Jr., H. A. Farach, and R. J. Creswick, *Superconductivity* (Academic Press, San Diego, 1995).
- ⁴² E. H. Brandt, Phys. Rev. B **55**, 14513 (1997).
- ⁴³ S. O. Valenzuela, (unpublished).